A MECHANICAL MODEL FOR THE GENERATION OF ARTIFICIAL SEISMOGRAMS

Andrej Umek[1]

SUMMARY

Accelerograms to simulate the shalow focus transform fault earthquakes are obtained on the basis of a mechanical model. Two semiinfinite elastic plates in the state of plane stress move tangentially to each other until the bond between them breaks because of excessive strains. The consecutive rebound motion of the plates produces synthetic seismograms. In the process of the mathematical analysis Fourier and Laplace transforms are applied to the equations of motion and the boundary conditions. The inversion is completed by the Cagniard-deHoop method, leading to the closed form results, shown graphically.

INTRODUCTION

To obtain a suitable input for a seismic analysis of a building one has to predict the possible ground motion at that particular site. For this purpose the earthquake-engineering practice offers two alternatives: the first is to take an actual accelerogram recorded at some other site, resembling at least in major characteristics the situation at the place of our interest; the other uses an artificial seismogram obtained by a modulation of the white noise as G.W. Housner and other authors did e.g. [1]. An artificial seismogram can however be obtained also from a mechanical model simulating the processes occurring in the earth crust during an earthquake. The main requirements imposed on such a mechanical model are that it should reproduce the generating mechanisms and the ground motion for at least one type of earthquake as closely as possible and at the same time retain mathematical tractability. Beside the model of the penny-shaped crack in an elastic solid [2] very few such models were explored in literature, which clearly shows the difficulties in satisfying the above mentioned demands.

According to plate tectonics the earthquakes occur mainly along the plate margines, which are of three basically different types: (1) constructive, where new crust is created, (2) destructive, where crust is consumed and (3) conservative, where crust is neither created nor destroyed. These are signified by transform faults. It is apparent that the earthquakes occurring at each type of plate boundary require different mechanical models. In this paper we are going to limit our attention to the earthquakes originating in transform faults. Here one plate is moving laterally to the other. If this motion is prevented at some part of the boundary, elastic energy starts accumulating in either plate. This process continues until the bond between the two plates ruptures due to the strains greater than the material can endure. At this moment the slip in the fault occurs and the accumulated strain-energy is released, which leads to the ground motion known as an earthquake. The mechanical model of this process is the topic of the present paper.

[1]Associate Professor, College of Engineering, University of Maribor, Maribor, Yugoslavia.

DESCRIPTION OF PROBLEM

The problem model shown in Fig. 1(a), consists of two semiinfinite elastic plates, which are assumed to be in the state of plane stress, and the transform fault which is a straight line. The plates are free to move in the directions shown, except for the part of the boundary of the length 2a where no relative motion of one plate against the other is possible. The problem model exhibits a symmetry with respect to the transform fault, therefore we are going to consider only its lower part shown in Fig. 1(b). A Cartesian coordinate system is introduced and the corresponding displacement components are denoted by u_1 and u_2. Thus the equations of motion become [3]:

$$\mu u_{\alpha,\beta\beta} + \left(\mu + \frac{2G\lambda}{\lambda+2G}\right) u_{\beta,\alpha\beta} = \rho \ddot{u} \qquad (1)$$

where the indices and take on values 1 and 2 respectively. Their repetition denotes summation and the comma partial differentiation. G and are Lamè constants and is the density of the material. With respect to time the whole problem is devided into two phases. During the first the two plates are connected with one another on the part of x_1-axis where $|x_1| < a$, and are moving along the x_1-axis in oposite directions. It is assumed that this motion is so slow that the problem is a statical one. Therefore the strains and stresses in the plate in Fig. 1(b) are determined by the following boundary conditions:

$$\begin{aligned} &\text{on } x_1 : \tau_{22} = 0;\ \tau_{12} = 0 \text{ for } |x_1| > a \text{ and } u_1 = 0 \text{ for } |x_1| < a \\ &\text{on } r \to \infty: u_1 = U,\ u_2 = 0 \end{aligned} \qquad (2)$$

where $r = (x_1^2 + x_2^2)^{1/2}$ and U is the displacement from the original unstrained position. We further assume, that at the end of the first phase, the material binding the two plates becomes plastified and stress distribution in it uniform. Neglecting the rigid body motion of the plates we obtain the equivalent boundary conditions describing the state in the plate at the end of phase one:

$$\begin{aligned} &\text{on } x_1 : \tau_{22} = 0;\ \tau_{12} = \left[H(x_1 + a) - H(x_1 - a)\right] \cdot \tau_o \\ &\text{on } r \to \infty: u_1 = 0,\ u_2 = 0 \end{aligned} \qquad (3)$$

where τ_o is the maximal shearing stress the plate material can sustain. At t=0 the bond between the two plates ruptures therefore both plates are free of any stresses along the x_1-axis and the second phase of the elastic rebound begins. It is characterized by the following boundary conditions

$$\begin{aligned} &\text{on } x_1 : \tau_{22} = 0;\ \tau_{12} = \tau_o \left[H(x_1 + a) - H(x_1 - a)\right]\left[1 - H(t)\right] \\ &\text{on } r \to \infty: u_1 = 0,\ u_2 = 0 \end{aligned} \qquad (4)$$

Since the main result of our investigation is to be the accel-

erations and not the displacements we are taking into account only the time-dependent part of the boundary conditions (4). Thus our problem is given by the equations of motion (1), the boundary conditions:

$$\text{on } x_1 : \tau_{22} = 0;\ \tau_{12} = -\tau_o\left[H(x_1 + a) - H(x_1 - a)\right]\cdot H(t) \qquad (5a)$$

$$\text{on } r \to \infty:\ u_1 = 0,\ u_2 = 0 \qquad (5b)$$

and the homogeneous initial conditions.

METHOD OF SOLUTION

Displacements are expressed with their potentials as

$$u_1 = \varphi_{,1} + \psi_{,2} \quad \text{and} \quad u_2 = \varphi_{,2} - \psi_{,1} . \qquad (6)$$

Introducing them into equations of motion (1) and boundary conditions (5a) yields:

$$\nabla^2\varphi = c_1^{-2}\,\ddot{\varphi}, \quad \nabla^2\psi = c_2^{-2}\,\ddot{\psi} \qquad (7)$$

and

$$2\varphi_{,11} - c_2^{-2}\,\ddot{\varphi} + \psi_{,12} = 0$$

$$2\varphi_{,12} - 2\psi_{,11} + c_2^{-2}\,\ddot{\psi} = -\frac{\tau_o}{G}\left[H(x_1 + a) - H(x_1 - a)\right] H(t) \qquad (8)$$

where

$$c_1^2 = \frac{2G}{\rho(1-\nu)}\ , \qquad c_2^2 = \frac{G}{\rho}\ , \qquad (9)$$

and ν is Poisson's ratio. Applying the Laplace transform in time and the Fourier transform in x_1 to the equations of motion (7) and boundary conditions (8), and taking into account homogeneous initial conditions, we obtain:

$$\tilde{\tilde{\varphi}}_{,22} - (\xi^2 + s_1^2)\,\tilde{\tilde{\varphi}} = 0\ , \quad \tilde{\tilde{\psi}}_{,22} - (\xi^2 + s_2^2)\,\tilde{\tilde{\psi}} = 0 \qquad (10)$$

and

$$(2\xi^2 + s_2^2)\,\tilde{\tilde{\varphi}} - i\xi\,\tilde{\tilde{\psi}}_{,2} = 0$$

$$2i\xi\,\tilde{\tilde{\varphi}}_{,2} + (2\xi^2 + s_2^2)\,\tilde{\tilde{\psi}} = -\frac{2\tau_o}{\xi s G}\sin(a\xi) \qquad (11)$$

where $s_1 = s/c_1$ and $s_2 = s/c_2$. The equations of motion (10) have become ordinary differential equations, which can be easily solved satisfying the boundary conditions (11) and (5b), and yield:

$$\tilde{\tilde{\varphi}} = \frac{2i\tau_o}{Gs}\,\frac{\beta}{\Delta}\sin(a\xi)\,\exp(-\alpha y)$$

$$\tilde{\tilde{\psi}} = -\frac{2\tau_o\,(2\xi^2 + s_2^2)}{Gs\xi\Delta}\sin(a\xi)\,\exp(-\beta x_2) \qquad (12)$$

where

$$\alpha = \sqrt{\xi^2 + s_1^2}\,, \quad \beta = \sqrt{\xi^2 + s_2^2} \quad \text{and} \quad \Delta = (2\xi^2 + s_2^2)^2 - 4\xi^2\alpha\beta \tag{13}$$

By transforming equations (6) and by introducing into them equations (12) we obtain the displacement components in the transformed domain as:

$$\tilde{u}_1 = -\frac{2\tau_o \sin(a\xi)}{sG}\left[\frac{\xi\beta}{\Delta}\exp(-\alpha x_2) - \frac{\beta(2\xi^2 + s_2^2)}{\xi\Delta}\exp(-\beta x_2)\right]$$

$$\tilde{u}_2 = -\frac{2i\tau_o \sin(a\xi)}{sG}\left[\frac{\alpha\beta}{\Delta}\exp(-\alpha x_2) - \frac{(2\xi^2 + s_2^2)}{\Delta}\exp(-\beta x_2)\right] \tag{14}$$

The above equations have to be transformed back into the real time and space domain. This process is started with the inverse Fourier transform yielding:

$$\bar{u}_1 = \frac{-\tau_o}{\pi sG}\int_{-\infty}^{\infty}\left[\frac{\xi\beta}{\Delta}\exp(-\alpha x_2) - \frac{\beta(2\xi^2 + s_2^2)}{\xi\Delta}\exp(-\beta x_2)\right]\sin(a\xi)\, e^{ix_1\xi}\, d\xi$$

$$\bar{u}_2 = \frac{-\tau_o}{\pi sG}\int_{-\infty}^{\infty}\left[\frac{\alpha\beta}{\Delta}\exp(-\alpha x_2) - \frac{(2\xi^2 + s_2^2)}{\Delta}\exp(-\beta x_2)\right]\sin(a\xi)\, e^{ix_1\xi}\, d\xi \tag{15}$$

To evaluate the integrals we were left with after the inverse Fourier transform and at the same time make the inverse Laplace transform we are going to use Cagniard-deHoop method [4]. Thus we have to put equations (15) in the form, in which the variables will appear only in the arguments of the exponential functions. This can be achieved by the following change of variables:

$$\xi \to s_1\xi\ ; \quad \alpha \to s_1\alpha\,, \quad \alpha = \sqrt{\xi^2 + 1}\ ; \quad \beta \to s_1\beta\,, \quad \beta = \sqrt{\xi^2 + \varkappa^2}\,,$$

$$\varkappa = c_1/c_2 = \sqrt{\frac{2}{1 - \nu}}\ ; \quad \Delta \to s_1^4\Delta\,, \quad \Delta = (2\xi^2 + \varkappa^2)^2 - 4\xi^2\alpha\beta \tag{16}$$

yielding

$$s^2\bar{u}_1 = -\frac{\tau_o c_1}{2\pi i G}\left[\bar{J}_1(a) - \bar{J}_1(-a) - \bar{J}_2(a) + \bar{J}_2(-a)\right]$$

$$s^2\bar{u}_2 = -\frac{\tau_o c_1}{2\pi i G}\left[\bar{J}_3(a) - \bar{J}_3(-a) - \bar{J}_4(a) + \bar{J}_4(-a)\right] \tag{17}$$

where

$$J_1(a) = \int_{-\infty}^{\infty}\frac{\beta\xi}{\Delta}\exp\left[-s_1\alpha x_2 + is_1(x_1 + a)\xi\right]d\xi$$

$$J_2(a) = \int_{-\infty}^{\infty}\frac{\beta(2\xi^2 + \varkappa^2)}{\xi\Delta}\exp\left[-s_1\beta x_2 + is_1(x_1 + a)\xi\right]d\xi$$

$$J_3(a) = \int_{-\infty}^{\infty}\frac{\alpha\beta}{\Delta}\exp\left[-s_1\alpha x_2 + is_1(x_1 + a)\xi\right]d\xi$$

$$J_4(a) = \int_{-\infty}^{\infty}\frac{(2\xi^2 + \varkappa^2)}{\Delta}\exp\left[-s_1\beta x_2 + is_1(x_1 + a)\xi\right]d\xi \tag{18}$$

Simultaneous evaluation and inversion of the integrals (18) is performed by Cagniard-deHoop method. Since this method is known well enough, we give the final results only. First for the following integrals:

$$\frac{1}{2i} J_1(a) = \frac{c_1}{r} H(\tau - 1)\, \mathrm{Im}\left[\frac{\beta\xi}{\Delta}\left(i\cos\vartheta + \frac{\tau}{\sqrt{\tau^2 - 1}}\sin\vartheta\right)\right]$$

$$\frac{1}{2i} J_3(a) = \frac{c_1}{r} H(\tau - 1)\, \mathrm{Im}\left[\frac{\alpha\beta}{\Delta}\left(i\cos\vartheta + \frac{\tau}{\sqrt{\tau^2 - 1}}\sin\vartheta\right)\right] \qquad (19)$$

where for the integrals $J_1(a)$ and $J_3(a)$

$$\tau = \frac{c_1 t}{r}\ ;\quad r = \sqrt{(x_1 + a)^2 + x_2^2}\ ;\quad \cos\vartheta = \frac{(x_1 + a)}{r}\ ;\quad \sin\vartheta = \frac{x_2}{r}\ ;$$

$$\xi = i\tau\cos\vartheta + \sqrt{\tau^2 - 1}\sin\vartheta\ . \qquad (20)$$

The evaluation of the other two integrals is rather more complicated. This is due to the fact that they represent the S - waves that originate directly from the stress distribution along the x_1 - axis and from the reflection of the P - waves from the fault. Thus we obtain:

$$\frac{1}{2i} J_2(a) = \frac{c_1}{r} H(\tau - \varkappa)\, \mathrm{Im}\left[\frac{\beta(2\xi^2 + \varkappa^2)}{\xi\Delta}\left(i\cos\vartheta + \frac{\tau}{\sqrt{\tau^2 - \varkappa^2}}\sin\vartheta\right)\right]$$
$$+ \frac{c_1}{r} f_\vartheta\, f_\tau\, \mathrm{Im}\left[\frac{\sqrt{\varkappa^2 - \eta^2}\,(\varkappa^2 - 2\eta^2)}{\Gamma\eta}\left(\cos\vartheta + \frac{\tau}{\sqrt{\tau^2 - \varkappa^2}}\sin\vartheta\right)\right]$$

$$\frac{1}{2i} J_4(a) = \frac{c_1}{r} H(\tau - \varkappa)\, \mathrm{Im}\left[\frac{(2\xi^2 + \varkappa^2)}{\Delta}\left(i\cos\vartheta + \frac{\tau}{\sqrt{\tau^2 - \varkappa^2}}\sin\vartheta\right)\right]$$
$$+ \frac{c_1}{r} f_\vartheta\, f_\tau\, \mathrm{Im}\left[\frac{(\varkappa^2 - 2\eta^2)}{\Gamma}\left(\cos\vartheta + \frac{\tau}{\sqrt{\tau^2 - \varkappa^2}}\sin\vartheta\right)\right] \qquad (21)$$

where τ, r, $\cos\vartheta$ and $\sin\vartheta$ are given by equations (20). The other quantities however are:

$$\xi = i\tau\cos\vartheta + \sqrt{\tau^2 - \varkappa^2}\sin\vartheta\ ,\quad \eta = \tau\cos\vartheta - \sqrt{\varkappa^2 - \tau^2}\sin\vartheta\ ,$$

$$\Gamma = (\varkappa^2 - 2\eta^2)^2 + 4i\eta\sqrt{\eta^2 - 1}\sqrt{\varkappa^2 - \eta^2}\ ,\quad f_\vartheta = H(|\varkappa\cos\vartheta| - 1)\ ,$$

$$f_\tau = H(\tau - \sqrt{\varkappa^2 - 1}\sin\vartheta - \cos\vartheta) - H(\tau - \varkappa) \qquad (22)$$

This completes the inversion of equations (17) yielding:

$$\ddot{u}_1 = -\frac{\tau_o c_1}{\pi G}\left[J_1(a) - J_1(-a) - J_2(a) + J_2(-a)\right]$$

$$\ddot{u}_2 = -\frac{\tau_o c_1}{\pi G}\left[J_3(a) - J_3(-a) - J_4(a) + J_4(-a)\right] \qquad (23)$$

RESULTS AND CONCLUSIONS

Equations (23) enable us to compute the x_1- and x_2-components of the acceleration as functions of time for any point in the half plane. The results depend on several parameters. It is therefore convenient to normalize the problem as follows: all distances are

normalized by the length of the bond between the two plates; a unit time is that required for an S-wave to travel a unit distance; and a unit mass is that of a unit cube of the plate material. With respect to these dimensionless units, the shear modulus, density and the shear wave velocity are all unity. In addition to the shear modulus the elastic properties of the plate material are defined by Poisson's ratio, which is taken to be 0.25. We further notice that the resulting accelerations are directly proportional to the shearing stress τ_0, to which the unit value is assigned in all our clculations.

After the normalization described above, we are left with only one parameter, which can still be varied, and this one is the dimensionless position of the recording point. For the presentation in this paper we have selected two recording points, given by the coordinates (3.0, 2.0) and (2.0, 3.0) and shown in Fig. 2(a) and Fig. 2(b) respectively. At both recording points the x_1-component of the acceleration is given. Two recording points are chosen because the semiinfinite plate can be devided, with respect to its response, into two sectors: in the first we have three distinct wave types i.e. P-waves, head waves, which are produced by the interaction of the P-waves with the fault, and S-waves. The recording point (3.0, 2.0) lies in this sector; the second sector, represented by the recording point (2.0, 3.0), exhibits only two distinct wave types. These are P- and S-waves.

Comparing the accelerograms shoen in Fig. 2(a) and 2(b) with the accelerograms of some actual earthquakes e.g. [5], we notice that the former exhibit fewer peaks. This is the consequence of simplifying assumptions, built into our model. The first, that the two semiinfinite plates are in the state of plane stress, leads to a nondispersive model, where a disturbance can propagate only with two distinct velocities. So the outgoing wave profiles change only slightly with the distance. The conditions in the earth crust however are dispersive and the wave profiles are changed as they progress. Owing to this process single peaks desintegrate thus creating a greater number of peaks. In order to obtain a better model taking into account the dispersive effects of the earth crust, we would have to proceed from our two-dimensional model to a three-dimensional one. Here however the mathematical tractability becomes the main problem. So any such improvement remains open to further research.

Since the time history of the fault slip accompanying an actual earthquake is not known well enough, the second simplifying assumption of the instantaneous separation of the plates has been made. Fig. 2(a) and 2(b) show that the peaks coincide with the arrival times of P-, head and S-waves emanating from the begining and the end of the load along the x_1-axis. This clearly demonstrates that the time history of the plate separation considerably influences the resulting accelerogram. The assumption, for example, that the time history of the plate separation is stepwise would result in accelerograms exhibiting for each step as many peaks as the accelerograms in Fig. 2(a) and 2(b) do, and thus yield a picture much closer to actual seismograms. Therefore the problem of the nature-true separation history becomes the key issue for further improvement of the presented model.

REFERENCES

[1] Jennings, P.S., Housner, G.W., and Tsai, N.C., Simulated Earthquake Motions, Earthquke Engineering Research Laboratory, California Institute of Technology, Apr. 1968.

[2] Housner, G.W., and Hudson, D.E., "The Port Hueneme Earthquake of March 18, 1957," Bull. Seism. Soc. Am., Vol. 48, No. 2, 1958.

[3] Achenbach, J.D., Wave Propagation in Elastic Solids, North-Holland, 1975, pp. 58 - 59.

[4] Fung, Y.C., Foundations of Solid Mechanics, Prentice-Hall, 1965, pp. 218 -224.

[5] Wiegel, R.L. ed., Earthquake Engineering, Prentice-Hall, 1970, pp. 78 – 80.

FIGURES

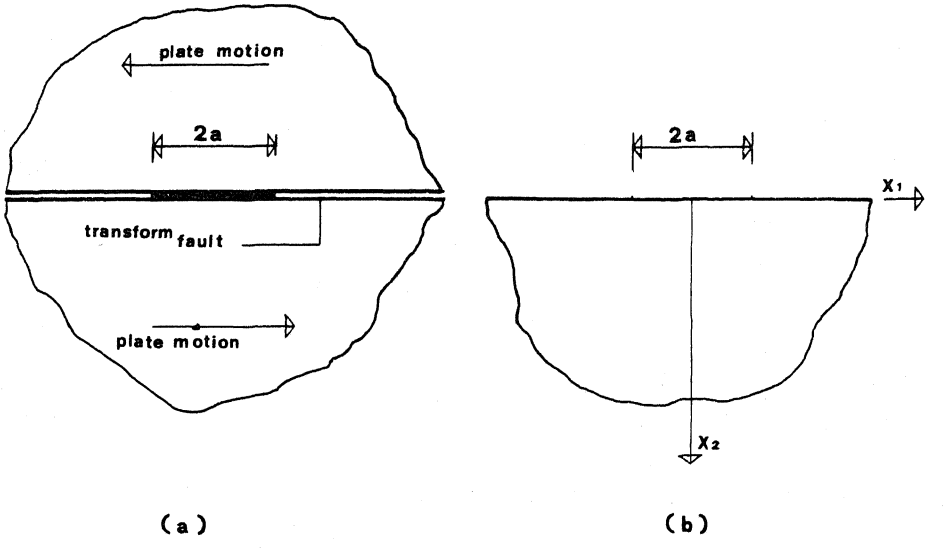

Figure 1. Problem Geometries: (a) Original Model; (b) Equivalent Model.

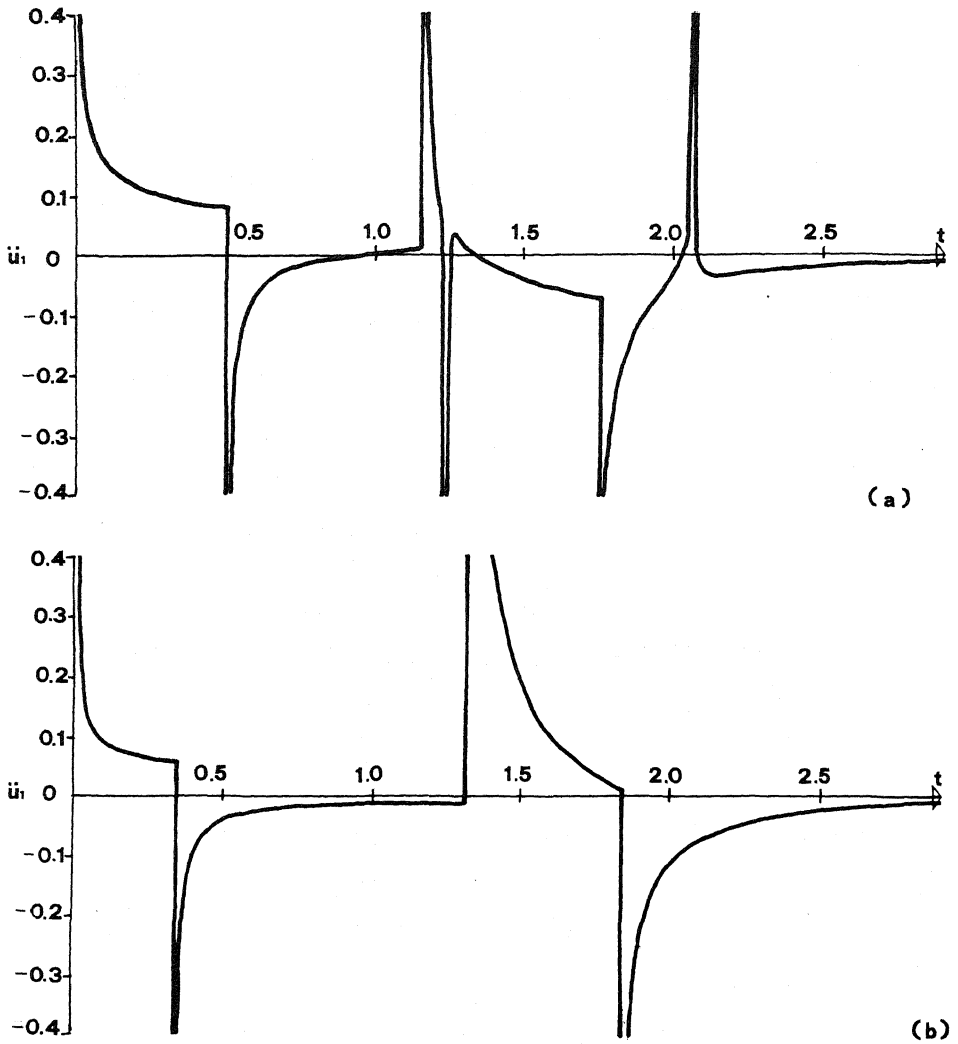

Figure 2. The x_1-components of Acceleration: (a) Recording Point (3.0, 2.0); (b) Recording Point (2.0, 3.0).